Effect of ion species on the accumulation of ion-beam damage in GaN

S. O. Kucheyev,* J. S. Williams, and C. Jagadish
Department of Electronic Materials Engineering, Research School of Physical Sciences and Engineering, The Australian National University, Canberra, ACT 0200, Australia

J. Zou
Electron Microscope Unit and Australian Key Center for Microscopy and Microanalysis, The University of Sydney, Sydney, NSW 2006, Australia

G. Li
Ledex Corporation, No. 9, Ta-Yio First Street, Ta-Fa Industrial District, Kaohsiung County, Taiwan, Republic of China

A. I. Titov
Department of Physical Electronics, St. Petersburg State Technical University, St. Petersburg 195251, Russia
(Received 5 February 2001; published 20 June 2001)

Wurtzite GaN epilayers bombarded with a wide range of ion species (10 keV ^{1}H, 40 keV ^{12}C, 50 keV ^{16}O, 600 keV ^{28}Si, 130 keV ^{63}Cu, 200 keV ^{107}Ag, 300 keV ^{197}Au, and 500 keV ^{209}Bi) are studied by a combination of Rutherford backscattering/channeling (RBS/C) spectrometry and cross-sectional transmission electron microscopy. Results show that strong dynamic annealing processes lead to a complex dependence of the damage-buildup behavior in GaN on ion species. For room-temperature bombardment with different ion species, bulk disorder, as measured by RBS/C, saturates at some level that is below the random level, and amorphization proceeds layer-by-layer from the GaN surface with increasing ion dose. The saturation level of bulk disorder depends on implant conditions and is much higher for light-ion bombardment than for the heavy-ion irradiation regime. In the case of light ions, when ion doses needed to observe significant lattice disorder in GaN are large ($\gtrsim 10^{16}\,\mathrm{cm}^{-2}$), chemical effects of implanted species dominate. Such implanted atoms appear to stabilize an amorphous phase in GaN and/or to act as effective traps for ion-beam-generated mobile point defects and enhance damage buildup. In particular, the presence of a large conce ntration of carbon in GaN strongly enhances the accumulation of implantation-produced disorder. For heavier ions, where chemical effects of implanted species seem to be negligible, an increase in the density of collision cascades strongly increases the level of implantation-produced lattice disorder in the bulk as well as the rate of layer-by-layer amorphization proceeding from the surface. Such an increase in stable damage and the rate of planar amorphization is attributed to (i) an increase in the defect clustering efficiency with increasing density of ion-beam-generated defects and/or (ii) a superlinear dependence of ion-beam-generated defects, which survive cascade quenching, on the density of collision cascades. Physical mechanisms responsible for such a superlinear dependence of ion-beam-generated defects on collision cascade density are considered. Mechanisms of surface and bulk amorphization in GaN are also discussed.

DOI: 10.1103/PhysRevB.64.035202 PACS number(s): 61.72.Cc, 61.72.Dd, 61.72.Yx, 68.55.Ln

I. INTRODUCTION

Significant technological importance of GaN has been an effective driving force for research interest in this material. Indeed, as discussed in a number of recent reviews on this topic,[1] GaN is finding applications in the fabrication of a range of electronic and photonic devices. In addition, research interest in GaN has been supported by interesting and somewhat unusual properties of this material.

Ion-beam disordering of GaN is an example of such physically interesting and technologically important research. Recent ion-implantation studies[2–18] have revealed that, unlike the situation for mature semiconductors such as Si and GaAs, GaN exhibits a range of intriguing behavior involving extreme property changes under ion bombardment.[19] In particular, it has been shown that dynamic annealing processes (i.e., defect-interaction processes) in GaN are extremely efficient even during heavy-ion bombardment at liquid-nitrogen temperature. As discussed in detail in Refs. 12 and 19, ion-beam-generated Frenkel pairs, which survive very fast quenching of collision cascades, are mobile in GaN even at liquid-nitrogen temperature, and most of them experience annihilation. In such a case of very efficient dynamic annealing, the damage-buildup behavior becomes rather complex, typically involving nucleation-limited amorphization.

Damage processes in GaN are also complicated by ion-beam-induced material dissociation.[13,14] Indeed, after amorphization of GaN, ion bombardment has been shown to result in material dissociation with the formation of N_2 gas bubbles embedded into a Ga-rich matrix of amorphous GaN. Such dramatic decomposition has been attributed to ion-beam-induced stoichiometric imbalance. In addition, high plasticity (and extremely low hardness) of amorphous GaN compared to that of crystalline GaN (Ref. 18) seems to aid the process of the formation and agglomeration of N_2 gas bubbles in GaN during ion bombardment.[16]

 ©2001 The American Physical Society

TABLE I. Implant conditions used in this study. Calculated values of the average number of lattice vacancies produced by one ion (N_{vac}^{tot}) and the number of vacancies in the maximum of the nuclear energy-deposition profile (N_{vac}^{max}) are also given.

Ion	Energy (keV)	Implantation temperature (°C)	Beam flux (10^{12} cm^{-2} s^{-1})	N_{vac}^{tot}	N_{vac}^{max} (vac/ion/Å)
$^{1}H^{-}$	10	−196	11	5	1.7×10^{-3}
$^{12}C^{-}$	40	−196, 20	14	236	0.23
$^{16}O^{-}$	50	−196, 20	19	338	0.36
$^{28}Si^{-}$	60	20	16	479	0.88
$^{63}Cu^{-}$	130	20	9.4	1240	2.18
$^{107}Ag^{+}$	200	20	0.6	1976	3.4
$^{197}Au^{+}$	300	−196	3.1	2956	5.7
$^{197}Au^{+}$	300	20	4.4	2956	5.7
$^{209}Bi^{+}$	500	−196, 20	~0.1	4646	5.9

Damage processes in GaN may also be complicated by anomalous ion-beam-induced surface erosion which occurs at elevated temperatures. For example, bombardment of GaN with 300 keV Au ions at 550 °C has been shown to result in the erosion of an ~1000-Å-thick surface layer.[15] Such efficient erosion during elevated-temperature ion bombardment may not only impose significant limitations on the technological applications of ''hot implants'' into GaN but also complicate the interpretation of experimental data, as has been discussed elsewhere.[15,19]

The above examples (of strong dynamic annealing, somewhat unexpected defect evolution, and ion-beam-induced material dissociation and anomalous surface erosion) clearly illustrate the complexity of ion-beam-damage processes in GaN. Such an unexpected (and certainly interesting) behavior imposes significant limitations on the technological applications of ion implantation in the fabrication of GaN-based devices. Hence, it is important to undertake systematic studies of ion-beam-damage processes in this material if potential applications are to be fully exploited.

In this paper, we report on a systematic study of the influence of ion species (using a range of ion species from ^{1}H to ^{209}Bi) on the damage-buildup behavior in GaN. We discuss chemical effects of implanted species. Such effects of enhanced damage accumulation and/or stabilization of an amorphous phase dominate in the case of light ions, where large ion doses are needed to produce significant lattice disorder to study the damage-buildup and amorphization behavior. Analyzing experimental data for ions of different masses and taking chemical effects into account, we discuss the effect of the density of collision cascades on implantation-produced lattice defects.

II. EXPERIMENT

The ~2-μm-thick wurtzite undoped GaN epilayers used in this study were grown on *c*-plane sapphire substrates by metalorganic chemical-vapor deposition (MOCVD) in a rotating-disk reactor at Ledex Corporation. Implantation was carried out over a wide dose range under conditions indicated in Table I, using the ANU 180 kV ion implanter and an ANU 1.7 MV tandem accelerator (NEC, 5SDH-4). During implantation, samples were tilted by ~7° relative to the incident ion beam to minimize channeling.

After implantation, samples were taken from the implanter chamber and characterized *ex situ* at room temperature by Rutherford backscattering/channeling (RBS/C) spectrometry using an ANU 1.7 MV tandem accelerator (NEC, 5SDH) with 1.8 MeV $^{4}He^{+}$ ions incident along the [0001] direction and backscattered into a detector at 98° relative to the incident beam direction. This glancing-angle detector geometry was used to provide enhanced depth resolution for examining near-surface damage accumulation. Selected samples were studied by cross-sectional transmission electron microscopy (XTEM) in a Philips CM12 transmission electron microscope operating at 120 keV. XTEM specimens were prepared by 3 keV Ar^{+} ion-beam thinning using a Gatan precision ion-polishing system.

III. RESULTS

Figures 1–6 show RBS/C spectra illustrating the damage buildup in GaN with increasing ion dose for implantation

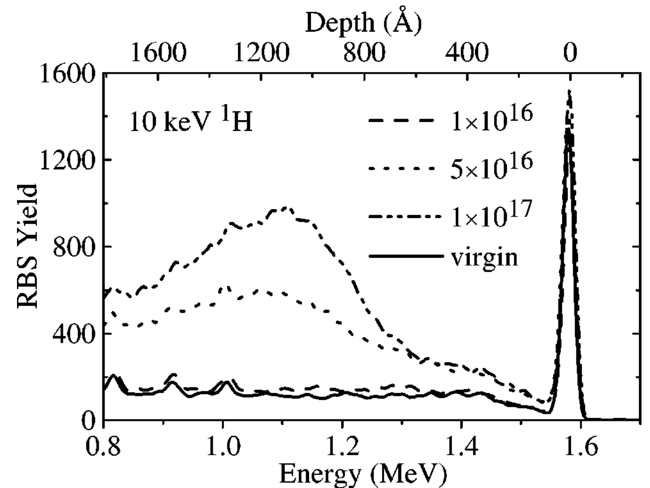

FIG. 1. RBS/C spectra showing the damage buildup for 10 keV H ion bombardment of GaN at −196 °C with a beam flux of 1.1×10^{13} cm^{-2} s^{-1}. Implantation doses (in cm^{-2}) are indicated in the figure. The random yield corresponds to ~5200 counts.

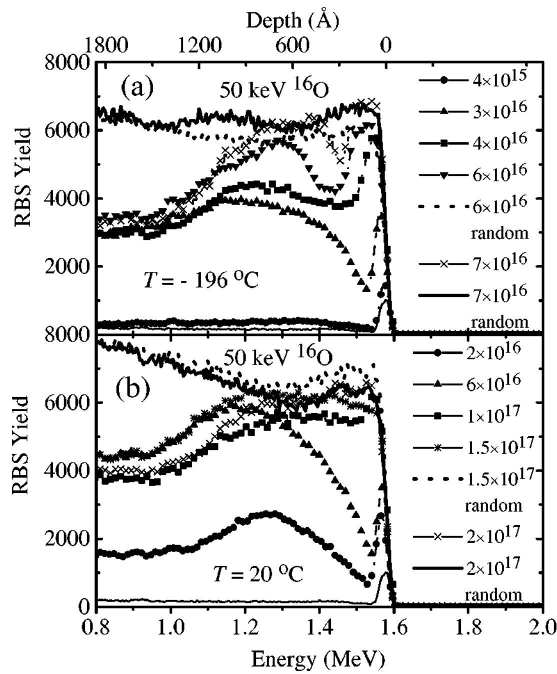

FIG. 2. RBS/C spectra showing the damage buildup for 50 keV O ion bombardment of GaN at $-196\,°C$ (a) and $20\,°C$ (b) with a beam flux of $1.9\times10^{13}\ cm^{-2}\,s^{-1}$. Implantation doses (in cm^{-2}) are indicated in the figure. A virgin spectrum is also shown for comparison.

with 10 keV H ions at $-196\,°C$ (Fig. 1), 50 keV O ions at -196 and $20\,°C$ (Fig. 2), 60 keV Si ions at $20\,°C$ (Fig. 3), 130 keV Cu ions at $20\,°C$ (Fig. 4), 200 keV Ag ions at $20\,°C$ (Fig. 5), and 500 keV Bi ions at -196 and $20\,°C$ (Fig. 6). Below, we discuss the results for each ion species separately. In addition, a detailed RBS/C and XTEM study of damage buildup in GaN under bombardment with 40 keV C and 300 keV Au ions at 20 and $-196\,°C$ was presented in Ref. 12. We will use data from Ref. 12 in the discussion and analysis

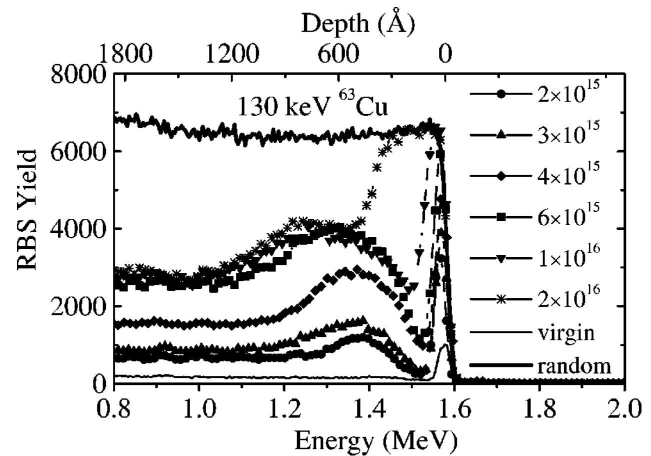

FIG. 4. RBS/C spectra showing the damage buildup for 130 keV Cu ion bombardment of GaN at $20\,°C$ with a beam flux of $9.4\times10^{12}\,cm^{-2}\,s^{-1}$. Implantation doses (in cm^{-2}) are indicated in the figure.

of the effect of ion species on damage buildup presented below.

It should be noted that, in the case of low-temperature implantation experiments reported here and in Ref. 12, some thermal annealing of ion-beam-produced lattice damage may have occurred during warming the low-temperature-implanted samples up to room temperature before the subsequent RBS/C or XTEM analysis. For example, such an effective room-temperature annealing of lattice damage produced by low-temperature bombardment has been found to occur in SiC.[20] However, in contrast to this situation in SiC, one might not expect a pronounced thermal annealing at room temperature of implantation-produced disorder in GaN. Indeed, due to very efficient dynamic annealing that occurs in GaN even at liquid-nitrogen temperature, a large part of ion-beam-generated point defects exhibits annihilation, and only more stable (energetically favorable) defect structures form in the lattice and effectively accumulate with increasing

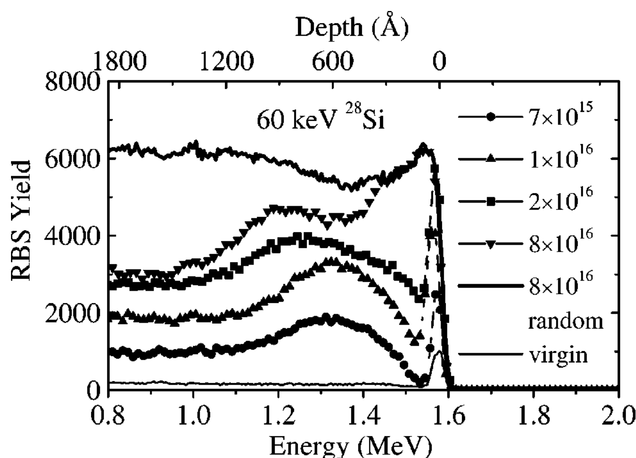

FIG. 3. RBS/C spectra showing the damage buildup for 60 keV Si ion bombardment of GaN at $20\,°C$ with a beam flux of $1.6\times10^{13}\,cm^{-2}\,s^{-1}$. Implantation doses (in cm^{-2}) are indicated in the figure.

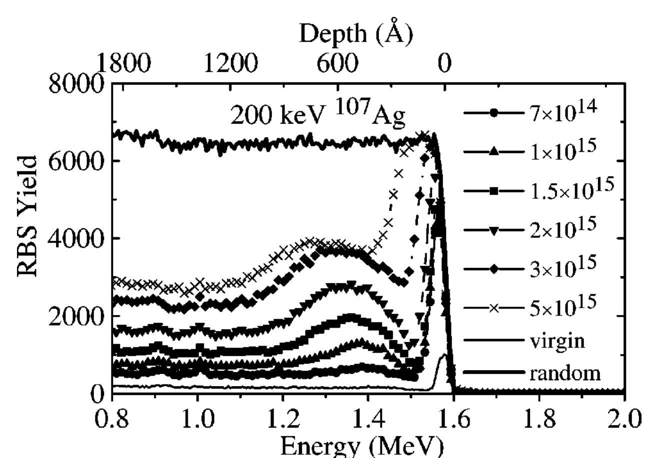

FIG. 5. RBS/C spectra showing the damage buildup for 200 keV Ag ion bombardment of GaN at $20\,°C$ with a beam flux of $6.0\times10^{11}\,cm^{-2}\,s^{-1}$. Implantation doses (in cm^{-2}) are indicated in the figure.

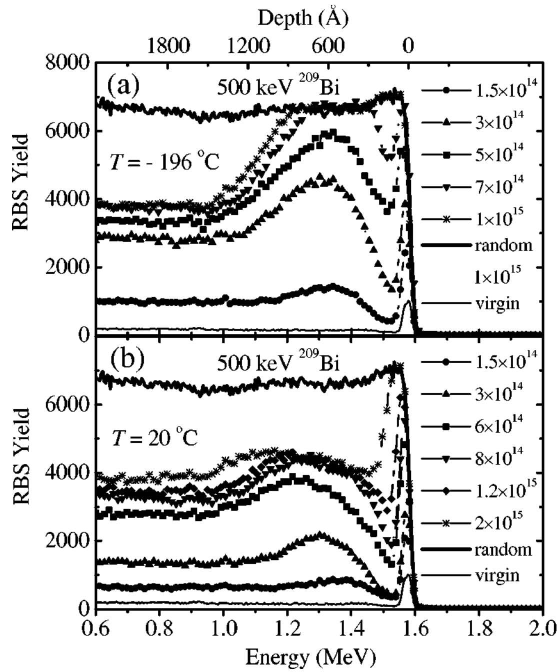

FIG. 6. RBS/C spectra showing the damage buildup for 500 keV Bi ion bombardment of GaN at $-196\,^{\circ}\mathrm{C}$ (a) and $20\,^{\circ}\mathrm{C}$ (b) with a beam flux of $\sim 1\times 10^{11}\,\mathrm{cm}^{-2}\,\mathrm{s}^{-1}$. Implantation doses (in cm^{-2}) are indicated in the figure.

ion dose. Our assumption in this work that the complex defect structures produced by ion bombardment at low temperatures will be thermally stable during annealing up to room temperature is supported by previous *in situ* RBS/C studies by Jiang *et al.*[7,8] These authors have shown that no detectable recovery of damage produced in GaN by bombardment with ^{16}O or ^{197}Au ions at $\sim -90\,^{\circ}\mathrm{C}$ occurs as a result of prolonged annealing at room temperature. However, additional experimental work (such as *in situ* RBS/C studies) is clearly desirable to study a possible room-temperature thermal recovery of damage produced in GaN by ion bombardment at liquid-nitrogen temperature.

A. Hydrogen

Figure 1 shows that the accumulation of implantation-produced lattice disorder in GaN during bombardment with 10 keV H ions at $-196\,^{\circ}\mathrm{C}$ becomes evident from RBS/C spectra only for rather large ion doses ($\gtrsim 1\times 10^{16}\,\mathrm{cm}^{-2}$). This is a direct consequence of very efficient dynamic annealing processes in GaN. However, for such large doses of species that form gas bubbles, the small direct-scattering peak seen in Fig. 1 for doses of 5×10^{16} and $1\times 10^{17}\,\mathrm{cm}^{-2}$ may have a contribution from a band of H_2 gas bubbles,[21] in addition to implantation-produced lattice defects. In favor of such a scenario is the fact that the maximum of the bulk RBS/C peak seen in Fig. 1 is at ~ 1100 Å. This is closer to the projected range of 10 keV ^{1}H ions (~ 1000 Å) rather than to the maximum of the nuclear energy-loss profile of these ions (~ 910 Å).[22] It is also seen from Fig. 1 that even the largest dose bombardment ($1\times 10^{17}\,\mathrm{cm}^{-2}$ of 10 keV H ions) results in only a slight increase in the magnitude of the surface defect peak, which reflects the accumulation of lattice defects at the surface. Hence, in the case of very light ions (such as ^{1}H), damage-accumulation studies using RBS/C are not possible in GaN bombarded even at liquid-nitrogen temperature and with low ion energies (such as 10 keV) because extremely large ion doses are needed to produce lattice disorder to levels detectable by RBS/C. For such large ion doses, the formation of H_2 gas bubbles hinders studies of lattice disorder. Hence, we will not further discuss data from Fig. 1 in the following analysis of the damage buildup in GaN.

B. Oxygen

Figure 2(a) shows that the main features of the damage-buildup behavior during bombardment of GaN with 50 keV O ions at $-196\,^{\circ}\mathrm{C}$ are similar to those previously reported for bombardment with 40 keV C, 100 and 300 keV Au ions,[12] as well as 500 keV Bi ions at $-196\,^{\circ}\mathrm{C}$ [see Fig. 6(a)]. Indeed, as is seen from Fig. 2(a), damage accumulation at $-196\,^{\circ}\mathrm{C}$ is bimodal with a strong surface-defect peak in addition to the bulk peak of disorder close to the maximum of the nuclear energy-loss profile. In this case, the damage buildup is sigmodal with ion dose, again consistent with previous results for C implantation,[12] where an amorphous phase nucleates both at the surface and in the bulk. Such a structure with surface and bulk amorphous layers is consistent with the RBS/C spectra illustrated in Fig. 2(a) in the case of doses of 6×10^{16} and $7\times 10^{16}\,\mathrm{cm}^{-2}$. With increasing ion dose, these two amorphous layers (in the bulk and at the surface) expand until they meet each other, resulting in a relatively thick, continuous surface layer of an amorphous material.

Figure 2(b) illustrates the damage buildup for bombardment of GaN with 50 keV O ions at $20\,^{\circ}\mathrm{C}$. It is seen that, again similar to the situation for ^{12}C (see Ref. 12), damage accumulation is bimodal. However, in contrast to the case of 40 keV C ion bombardment [see Fig. 1(b) in Ref. 12], implantation with O ions at $20\,^{\circ}\mathrm{C}$ does not appear to result in bulk amorphization. Instead, bulk disorder saturates at a level (which is at $\sim 85\%$ of the random level), which is, however, much higher than the saturation level for the case of bombardment with heavier ions [see Figs. 3, 5, 6(b), and Ref. 12]. We will return to the discussion of this fact below.

Similar to the situation for ^{1}H (discussed above) and ^{12}C (discussed in Ref. 12), the study of damage buildup in GaN exposed to implantation with ^{16}O ions is complicated by the fact that ion doses necessary to amorphize GaN with these ions are extremely large even in the case of bombardment at liquid-nitrogen temperature. This is clearly illustrated in Figs. 2(a) and 2(b), where, for large ion doses, both channeling and random spectra are given. It is seen from Figs. 2(a) and 2(b) that the height (and the shape) of random spectra changes with increasing ion dose above $\sim 5\times 10^{16}\,\mathrm{cm}^{-2}$, which corresponds to several at. % of O atoms implanted into the GaN matrix. Moreover, relative to the energy scale, the depth scale in RBS/C spectra also changes with increasing ion dose due to the changes in the energy losses of the analyzing α particles (see Ref. 12 for a more detailed dis-

cussion of this effect). In the case of such high ion doses, a quantitative estimation of the concentration vs depth profiles of implantation-produced lattice disorder from RBS/C spectra becomes a rather challenging problem.

C. Silicon

Shown in Fig. 3 are RBS/C spectra illustrating the buildup of lattice disorder in GaN implanted with 60 keV Si ions at room temperature. It is seen that, in this case of intermediate-mass ions, the behavior of damage buildup with increasing ion dose is similar to that previously observed for heavy-ion (^{197}Au) bombardment at room temperature.[8,12] Indeed, Fig. 3 illustrates a bimodal damage buildup with evidence for defect saturation rather than amorphization in the crystal bulk for high ion doses. In this case, amorphization only appears to proceed layer-by-layer from the surface with increasing ion dose. It is interesting that, similar to bombardment with ^{16}O ions discussed above, the bulk damage level attained at high doses of ^{28}Si ions (see Fig. 3) is larger than the saturation level of damage in the case of irradiation with ^{197}Au ions (see Ref. 12). In addition, due to the fact that relatively large Si ion doses are required for amorphization of GaN at 20 °C ($\gtrsim 5\times10^{16}$ cm^{-2}), the chemical effects of implanted Si atoms may also affect the damage buildup, as will be discussed more fully below. Such a large concentration of implanted
Si atoms (with, presumably, precipitation of Si) is also responsible for a large dip in the RBS/C random spectrum (around ~500 Å) shown in Fig. 3 in the case of a dose of 8×10^{16} cm^{-2}.

D. Heavier ions: ^{63}Cu, ^{107}Ag, and ^{209}Bi

Damage buildup for heavier ions is illustrated in Figs. 4–6 for Cu, Ag, and Bi ion bombardment, respectively. A detailed RBS/C and XTEM study of the damage buildup in GaN under bombardment with 300 keV Au ions at −196 and 20 °C was presented in Ref. 12. Figures 4–6, as well as data for Au ion bombardment,[12] show quite a similar behavior of damage accumulation for all these heavier ions. Indeed, heavy-ion bombardment of GaN at 20 °C appears to result in amorphization which proceeds layer-by-layer from the surface, while disorder in the bulk saturates at some level which is below the random level (see Figs. 4–6 and Ref. 12). For implantation at −196 °C, the main features of the damage-buildup behavior are similar for all ion species used (both light and heavy), as was discussed in Sec. III B.

It should be noted that, in contrast to lighter ions, the doses required to study the amorphization behavior in GaN during bombardment with heavier ions at room temperature are relatively low. In this case, when maximum concentrations of implanted species are $\lesssim 1$ at. %, the chemical effects of implanted atoms appear to be negligible at least for the heavy-ion species used in this study, as will be shown below. Hence, an analysis of the damage-buildup behavior for these ions can assist an understanding of the effects of the density of collision cascades on implantation-produced lattice disorder in GaN. Such an analysis is presented in Sec. IV.

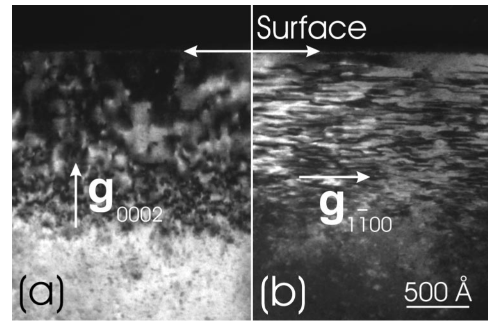

FIG. 7. Dark-field XTEM images [(a) **g**=0002* and (b) **g** =$1\bar{1}00$*] of the GaN epilayers bombarded at 20 °C with 60 keV Si ions with a beam flux of 1.6×10^{13} cm^{-2} s^{-1} to a dose of 2×10^{16} cm^{-2}.

E. Defect microstructure

The microstructure of lattice defects produced in GaN by bombardment with light 40 keV ^{12}C and heavy 100 and 300 keV ^{197}Au ions at −196 and 20 °C has previously been reported in Ref. 12. It has been shown that, with increasing dose of C or Au ions, damage evolution proceeds via the formation of point-defect complexes and a band of planar defects, which are parallel to the basal plane of the GaN film.[12] For completeness, in the present work we present results of a XTEM study of lattice defects produced in GaN by bombardment with intermediate-mass ions (^{28}Si).

Figure 7 shows dark-field images of GaN bombarded at 20 °C with 60 keV Si ions to a dose of 2×10^{16} cm^{-2}. These images indicate the presence of point-defect clusters [see the **g**=0002* image in Fig. 7(a)] and planar defects [see the **g** =$1\bar{1}00$* image in Fig. 7(b)] in the near-surface region damaged by ion bombardment (~1500 Å from the GaN surface). Hence, it can be concluded that these planar defects are characteristic for GaN bombarded to high ion doses with different ions (from very light, such as ^{12}C, to rather heavy, such as ^{197}Au). More detailed high resolution XTEM studies of the microstructure of these planar defects are in progress.

The sample from Fig. 7 (bombarded with Si ions) has also been studied by XTEM with the electron beam precisely parallel to the GaN surface to minimize edge effects on the contrast of the near-surface region. This study reveals the presence of a thin surface-amorphous layer which is ~40-Å-thick (figures are not shown), which is consistent with the strong surface defect peak seen from the RBS/C spectrum shown in Fig. 3. The formation of such surface amorphous layers (as well as amorphization proceeding layer-by-layer from the surface) has previously been attributed to the trapping of migrating point defects by the GaN surface or the amorphous/crystalline interface.[12] We will discuss this issue in more detail in Secs. IV C and IV D.

IV. DISCUSSION

A. Effect of ion species on damage buildup

All RBS/C spectra presented here and in Ref. 12 have been analyzed using one of the conventional algorithms[23] for extracting depth profiles of the effective number of scattering

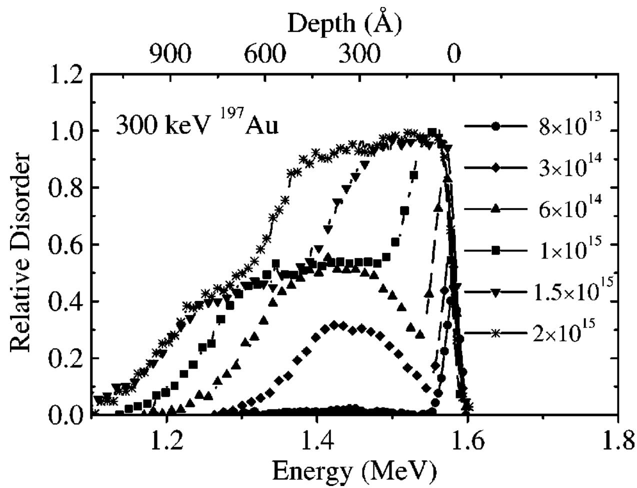

FIG. 8. The depth profiles of relative disorder in GaN films bombarded at 20 °C with 300 keV Au ions with a beam flux of $4.4\times10^{12}\,\mathrm{cm}^{-2}\,\mathrm{s}^{-1}$. Implantation doses (in cm^{-2}) are indicated in the figure. The original RBS/C data for these implants were given in Ref. 12.

centers. For brevity, the number of scattering centers extracted from RBS/C data, normalized to the atomic concentration of GaN, will be referred to below as ''relative disorder''. As an example, Fig. 8 illustrates depth profiles of relative disorder in GaN bombarded with 300 keV Au ions at 20 °C. This figure shows a damage-buildup behavior that is typical for heavy-ion bombardment of GaN at room temperature, as was discussed in Sec. III D.

Figure 9 illustrates the ion-dose dependence of maximum relative disorder in the bulk defect peak for implantation with seven different ions at room temperature. It is seen from this figure that, with increasing dose of heavy ions (^{63}Cu, ^{107}Ag, ^{197}Au, and ^{209}Bi), implantation-produced lattice damage in the bulk exhibits saturation, with the saturation level being $\sim0.4-0.5$ for all these heavy species. The difference in the saturation level for different heavy ions may be attributed to different type, concentration, and/or size of planar defects and point-defect complexes formed in the

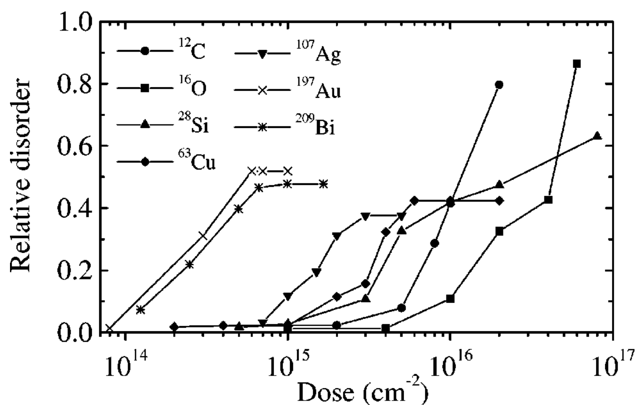

FIG. 9. Maximum relative disorder (extracted from RBS/C spectra) in the bulk defect peak as a function of dose for ions implanted at 20 °C, as indicated in the legend. See Table I for the details of implant conditions.

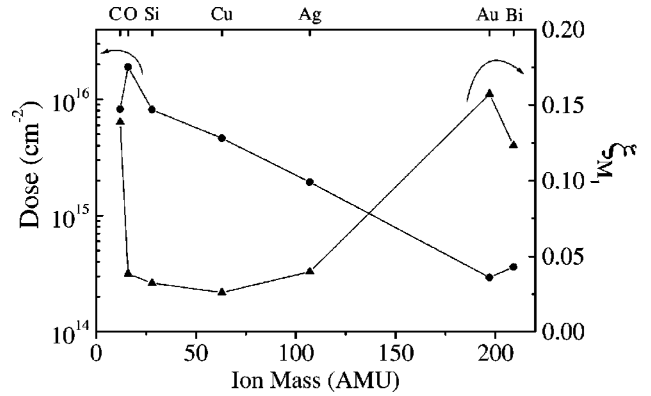

FIG. 10. Left axis: the ion-mass dependence of the ion dose necessary to produce relative disorder of 0.3 (as measured by RBS/C) by implantation at 20 °C. Right axis: the dependence of ξ_{M_1} ($\xi_{M_1}=$ the ratio of the level of lattice disorder measured experimentally to the damage level predicted based on ballistic calculations) on ion mass. See Table I for the details of implant conditions.

GaN lattice during bombardment under different implant conditions. For example, Fig. 9 shows a lower saturation level for the case of bombardment with Ag ions than with other heavy ions used. This fact appears to be due to a lower value of beam flux of Ag ions (see Table I). In contrast to the case of bombardment with heavy ions, Fig. 9 shows that the apparent saturation level for bombardment with lighter O and Si ions is significantly larger and in the case of C ion bombardment, no bulk damage saturation has been observed by RBS/C.[12] We attribute this result to dominating chemical effects of implanted light ions, as will be discussed in more detail below.

Figure 9 also shows that ion doses necessary to produce a particular level of relative disorder are different for different implants. This effect is better illustrated in Fig. 10 (the left axis), which shows the ion-mass dependence of the ion doses required to produce 30% relative disorder, $\Phi_{0.3}$. Such ion doses, $\Phi_{0.3}$, have been found by interpolation of damage-buildup curves from Fig. 9.[24] It is seen from Fig. 10 (the left axis) that $\Phi_{0.3}$ generally decreases with increasing ion mass. This qualitative trend is expected since the number of ion-beam-generated atomic displacements increases with ion mass. To support this assertion, the last two columns of Table I give results of TRIM calculations[25,26] of the number of lattice vacancies produced in GaN by the ion species used in this study.

However, two deviations from the trend expected are clearly seen in Fig. 10 for the cases of ^{12}C and ^{209}Bi ions. For example, $\Phi_{0.3}$ for ^{12}C ions is ~2.3 times smaller than $\Phi_{0.3}$ for ^{16}O ions, despite the fact that ^{16}O ions produce ~1.6 times more vacancies than ^{12}C ions in the maximum of the nuclear energy-loss profile (see Table I). This is a somewhat extreme example of chemical effects of implanted species, consistent with the data for C shown in Fig. 9, as will be discussed below. In addition to ^{12}C, irradiation with ^{209}Bi ions produced less stable lattice damage than bombardment with ^{197}Au ions, although ^{209}Bi ions generate a larger number of atomic displacements than ^{197}Au ions. However, this

result may be attributed to the lower beam-flux value in the case of Bi ions compared with the beam-flux value of Au ions (see Table I). Results reported previously[12,17] showed that the level of implantation-produced lattice disorder in GaN depended on ion beam flux. Indeed, with increasing beam flux, an increase in the density of ion-beam-generated point defects enhances interactions between such mobile point defects. This aids the process of formation of stable defect complexes. Hence, in addition to chemical effects and the effects of the density of collision cascades discussed below, beam-flux values must be taken into account for a correct interpretation of the influence of ion species on damage buildup.

Table I shows that, with an exception of Ag and Bi implants where much lower beam-flux values were used, the values of beam flux of different ion species were compatible with each other. Hence, given that the flux effect in GaN during ion bombardment at room temperature is not very strong,[12] we can neglect the influence of the difference in beam flux for different ions (except extreme cases of Ag and Bi) in the analysis of chemical effects and the effects of cascade density on the buildup of implantation-produced damage in GaN presented in this paper.

A further insight into the effect of ion mass on implantation-produced lattice disorder in GaN is given in Fig. 10 (the right axis), which shows the ion-mass dependence of ξ_{M_1}, the ratio of the level of lattice disorder of 0.3 (as measured by RBS/C) to the damage level predicted based on ballistic calculations[26] $\Phi_{0.3}N_{vac}^{max}/n_{at}$, where N_{vac}^{max} is the number of lattice vacancies in the maximum of the nuclear energy-loss profile (see Table I), and n_{at} is the atomic concentration of GaN. In the first approximation, the parameter ξ_{M_1} reflects the effectiveness of the production of stable lattice disorder (N^{def}) by ion bombardment under particular implant conditions: $N^{def}=\xi_{M_1}\Phi N_{vac}^{max}$ for relatively low levels of lattice disorder, where Φ is ion dose. If postimplantation stable lattice damage were the same as the one predicted based on ballistic calculations,[25] ξ_{M_1} would be equal to unity and independent of ion mass.

In contrast to such expectations, Fig. 10 (the right axis) shows a rather complex dependence of ξ_{M_1} on ion mass. First of all, for all ion species used, ξ_{M_1} is significantly below unity. This is a direct consequence of strong dynamic annealing processes when a large fraction of ion-beam-generated point defects experiences annihilation.[27] It is also seen from Fig. 10 (the right axis) that, with increasing ion mass from ^{12}C to ^{63}Cu, ξ_{M_1} decreases. For ions heavier than ^{63}Cu, ξ_{M_1} shows an increase with increasing ion mass.[28] An explanation for such an interesting behavior of ξ_{M_1} is given in the following sections.

B. Chemical effects

We attribute a decrease in ξ_{M_1} with increasing ion mass for light ions (from ^{12}C to ^{63}Cu) to dominating chemical effects due to relatively high concentrations of implanted species. Although the scale of such chemical effects depends on the particular ion species used, Figs. 9 and 10 indicate that all light ions used in this study (C, O, and Si) effectively enhance the buildup of implantation disorder. However, carbon exhibits the largest effect, as clearly shown in Figs. 9 and 10.

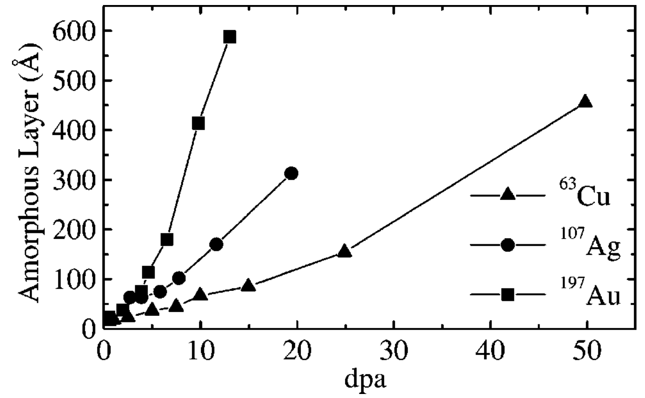

FIG. 11. The dependence of the thickness of surface-amorphous layers on DPA for bombardment of GaN with 130 keV Cu, 200 keV Ag, and 300 keV Au ions at 20 °C. See Table I for the details of implant conditions.

A chemical enhancement of damage buildup, as observed by RBS/C, can be due to (i) the trapping of ion-beam-generated migrating point defects by implanted impurity atoms, (ii) second phase formation and associated lattice distortion, and/or (iii) enhanced stability of irradiation-induced defects in GaN containing a high concentration of C, O, or Si. Indeed, trapping of migrating defects at impurity atoms may result in stable defect clusters that are observed as enhanced scattering centers in RBS/C or directly by XTEM. At high concentrations (above a few at. %), precipitation of a second phase involving the implanted atoms is increasingly likely, thus leading to disordering of the surrounding GaN matrix. Alternatively, large concentrations of implanted atoms may enhance the stability of an amorphous phase in GaN by defect trapping and/or influencing energy barriers for defect migration and interactions. Additional studies would be desirable to ascertain contributions to the chemical effect from each of the above three processes.

C. Surface amorphization

In this section, we discuss the main features of ion-beam-induced amorphization, which proceeds layer-by-layer from the GaN surface. Figure 11 illustrates the dose dependence of the thickness of surface amorphous layers in GaN bombarded with 130 keV Cu, 200 keV Ag, and 300 keV Au ions at 20 °C. In order to compare results obtained for different ion species, ion doses in Fig. 11 were multiplied by N_{vac}^{max}/n_{at}, and the product is shown as DPA (displacements per atom).[29] The thickness of surface amorphous layers shown in Fig. 11 has been determined from RBS/C spectra. An assumption was made in cases where the RBS/C surface peaks did not reach the random level that they originate from a completely disordered material at the surface. As discussed earlier in this paper (see Sec. III E), such an assumption has been supported by XTEM studies, especially in the case of

heavy-ion bombardment and relatively thick surface amorphous layers as shown in Fig. 11. The thickness of amorphous layers determined using this method is consistent with amorphous layer thickness determined for some samples using XTEM or directly from RBS/C spectra in the case of thick surface amorphous layers.

Figure 11 shows that the rate of planar amorphization (normalized to DPA) proceeding from the GaN surface increases with increasing ion mass. This may result from cascade-density effects, whereby defect clustering rather than annihilation is effectively enhanced, as will be discussed more fully in the following section. Interestingly, such a discussion will help us to better understand the influence of the density of collision cascades on ion-beam damage in GaN.

Figure 11 also shows that the thickness of surface-amorphous layers superlinearly depends on ion dose. This effect can be attributed to the fact that, with increasing ion dose, the amorphous/crystalline interface moves into a region with a larger level of defect generation by the ion beam. Alternatively, the fact that the amorphous/crystalline interface moves into a region with a larger level of implantation-produced lattice damage may also result in a superlinear dependence of the thickness of surface amorphous layers on ion dose if stable defects near the amorphous/crystalline interface aid the process of layer-by-layer amorphization.

Results also show that the amorphization rate increases with decreasing implantation temperature from 20 to $-196\,^{\circ}\mathrm{C}$ (figures are not shown). This is a typical behavior for ion-beam-induced epitaxial amorphization that occurs in different semiconductors under certain implant conditions.[30] However, at present, the micromechanism of layer-by-layer amorphization is still unknown. Even for Si, for which such a nonequilibrium phase transition has been studied most extensively,[31] an adequate model for ion-beam-induced epitaxial amorphization has not been developed, partly due to the complexity of this problem.

D. Role of collision-cascade density

In this section, we discuss the effect of the density of collision cascades on implantation-produced lattice disorder in GaN. The buildup of damage in the bulk, as characterized by the parameter ξ_{M_1}, is treated first. Figure 10 shows that ξ_{M_1} increases with increasing ion mass for heavy ions (^{63}Cu, ^{107}Ag, and ^{197}Au).[28] Amorphization studies in GaN bombarded with these heavier ions require relatively low ion doses. Hence, the chemical effects of implanted species appear to be negligible, and the ion-mass dependence of ξ_{M_1} should mainly reflect the effect of the density of collision cascades. Data from Fig. 10 show that an increase in the density of collision cascades strongly enhances the level of implantation-produced stable lattice disorder in GaN.[32] This effect can be attributed to an increase in the efficiency of clustering of mobile point defects into stable defect complexes with increasing density of ion-beam-generated point defects. Such an explanation is supported by the flux effect observed in GaN during heavy-ion bombardment.[12,17] Both cases, the cascade effect and the flux effect, may indicate that defect clustering efficiency increases with the rate of defect generation. It should be noted that an increase in the density of collision cascades should enhance the formation of stable defects even for implant conditions when the flux effect is weak. This is due to the fact that interaction processes between mobile point defects from the same collision cascade may occur in much shorter time intervals than migration and interaction of defects produced in different collision cascades.

An additional explanation for the strong dependence of implantation-produced stable lattice disorder in GaN on the density of collision cascades (revealed in Fig. 10) is a superlinear dependence of the concentration of ion-beam-produced point defects, which survive cascade quenching, on the density of collision cascades. This effect may be attributed to collective energy-spike processes that take place in dense collision cascades formed by heavy ions within very short time intervals of ~ 10 ps. These nonlinear energy-spike processes (such as displacement and/or thermal spikes) are well accepted in the literature in the case of Si,[33] the most extensively studied semiconductor, to explain the superlinear dependence of ion-beam-generated lattice disorder on cascade density.

Alternatively, the mass-dependent damage buildup may be due to a decrease in the effective displacement energy of atoms in the GaN matrix with increasing density of collision cascades. This effect may result from either the breaking of a large number of atomic bonds within a relatively small volume of a collision cascade or the reduced displacement energy of atoms with missing nearest neighbors, which arises due to a very high displacement density.[33] There may also be local material decomposition occurring within dense collision cascades, as has been discussed in more detail elsewhere.[12–14] Both these effects would also be expected to result in a superlinear dependence of ion-beam-generated defects on the density of collision cascades.

A superlinear dependence of the concentration of ion-beam-produced defects on cascade density discussed above appears to be supported by results from Fig. 11 (discussed in Sec. IV C), which shows that the rate of planar amorphization proceeding from the GaN surface also increases with increasing density of collision cascades. However, the process of surface-amorphization is rather complex. For example, the surface-amorphization behavior observed can be attributed to complex nonlinear disordering processes which favor clustering of ion-beam-generated defects at the amorphous/crystalline interface with increasing density of collision cascades. If such nonlinear defect accumulation at the amorphous/crystalline interface takes place, an increase in cascade density will also result in an increased rate of surface amorphization. Alternatively, an increase in the rate of surface amorphization with increasing density of collision cascades may be due to a decreased degree of lattice reordering during quenching of very dense collision cascades produced by heavy ions.[34] Indeed, in contrast to the situation in the crystal bulk, where cascades are surrounded by the crystal on all sides, the presence of an amorphous/crystalline interface may hinder the process of lattice reordering during cascade quenching. For example, if a dense collision cascade

behaves like a thermal spike, quenching and subsequent recrystallization of the resultant molten zone may be inhibited by the presence of an amorphous/crystalline interface. This effect might be expected to be enhanced as cascade density increases. As a result, this may lead to an increase in the rate of surface amorphization with increasing density of collision cascades.

It should also be noted that an increase in the rate of surface amorphization, with increasing density of collision cascades, revealed in Fig. 11, cannot be explained by a possible increase in the flux of point defects migrating from the bulk toward the surface or amorphous/crystalline interface. Indeed, although layer-by-layer amorphization is generally attributed to the trapping of such migrating point defects by the surface or amorphous/crystalline interface (see, for example, Ref. 12 and references therein), an increase in the defect clustering efficiency in the bulk, with increasing density of collision cascades, results in a decrease in the flux of point defects migrating from the bulk toward the surface and, hence, cannot account for the experimental data shown in Fig. 11. Moreover, such a long-range migration of point defects in GaN during ion irradiation appears to occur only for rather low ion doses (i.e., low levels of lattice disorder in the crystal). Indeed, an increased rate of surface amorphization in the case of ion bombardment using low beam fluxes (as illustrated in Figs. 5 and 11 in the case of Ag ion bombardment) occurs only for rather low ion doses. With increasing ion dose and, hence, the level of implantation-produced lattice disorder, effective diffusion lengths of point defects seem to decrease, presumably due to an increase in the probability of defect interactions and local clustering. However, it is clear that, at present, further studies are desirable to better understand the mechanism of planar amorphization and the physical processes responsible for the increase in implantation-produced stable lattice damage with increasing cascade density observed in this study.

E. Comparison with metals and other semiconductors

It should be noted that chemical enhancement of damage-buildup discussed above is, in fact, not new and has previously been found in both semiconductors and metals.[35,36] Indeed, chemical effects often dominate the damage-buildup behavior in an implantation regime with strong dynamic annealing when large ion doses are needed to observe significant disorder. Such strong dynamic annealing, which occurs in GaN even during heavy-ion bombardment at liquid-nitrogen temperature, is somewhat similar to the situation for most metals or even for mature semiconductors (such as Si and GaAs) during ion irradiation at elevated temperatures.

For example, in the case of implantation-produced damage in metals, it has been recognized that chemical effects of ion species implanted to large ion doses result in a reduced level of dynamic annealing and stabilization of an amorphous phase.[35] Most metals, particularly elemental metals, are impossible to amorphize even by heavy-ion bombardment at low temperatures without such a chemical stabilization of the amorphous phase. This experimental fact has previously been attributed to extremely efficient dynamic annealing processes in metals,[35] which is somewhat similar to the situation in GaN.

In the case of Si, bombardment with ^{12}C ions at room temperature has previously been shown to result in an enhanced damage accumulation compared to the case of irradiation with other light-ion species such as ^{11}B. This effect has been attributed to the formation of stable complexes of Si self-interstitials with C atoms.[36]

V. CONCLUSIONS

In conclusion, the damage-buildup and amorphization behavior in GaN bombarded with a wide range of ion species (see Table I) have been studied by a combination of RBS/C and XTEM techniques. In the case of light ions, when the ion doses needed to study the damage-buildup and amorphization behavior are large, chemical effects of implanted species result in an enhancement of damage-buildup. In particular, a strongly enhanced damage-buildup has been observed for bombardment with ^{12}C ions. In addition, results show that an increase in the density of collision cascades strongly increases the level of implantation-produced lattice disorder in the bulk. The rate of layer-by-layer amorphization proceeding from the surface also increases with increasing density of collision cascades. Such an increase in stable damage and the rate of surface amorphization has been attributed to (i) an increase in the defect clustering efficiency with increasing density of ion-beam-generated defects and (ii) a superlinear dependence of ion-beam-generated defects, which survive cascade quenching, on the density of collision cascades. Additional studies are needed to better understand the micromechanism of such a superlinear dependence of ion-beam-generated defects on collision cascade density.

ACKNOWLEDGMENT

J.Z. thanks the Australian Research Council for providing financial support.

*Email address: sergei.kucheyev@anu.edu.au

[1] See, for example, J. W. Orton and C. T. Foxon, Rep. Prog. Phys. **61**, 1 (1998); S. J. Pearton, J. C. Zolper, R. J. Shul, and F. Ren, J. Appl. Phys. **86**, 1 (1999); S. C. Jain, M. Willander, J. Narayan, and R. Van Overstraeten, *ibid.* **87**, 965 (2000), and references therein.

[2] H. H. Tan, J. S. Williams, J. Zou, D. J. Cockayne, S. J. Pearton, and R. A. Stall, Appl. Phys. Lett. **69**, 2364 (1996).

[3] C. Liu, B. Mensching, M. Zeitler, K. Volz, and B. Rauschenbach, Phys. Rev. B **57**, 2530 (1998).

[4] N. Parikh, A. Suvkhanov, M. Lioubtchenko, E. Carlson, M. Bremser, D. Bray, R. Davis, and J. Hunn, Nucl. Instrum. Methods Phys. Res. B **127/128**, 463 (1997).

[5] A. Suvkhanov, J. Hunn, W. Wu, D. Thomson, K. Price, N. Parikh, E. Irene, R. F. Davis, and L. Krasnobaev, in *Wide-Bandgap Semiconductors for High Power, High Frequency and High Temperature*, edited by S. DenBaars, J. Palmour, M. Shur, and M. Spencer, Mater. Res. Soc. Symp. Proc. No. **512** (Mate-

rials Research Society, Warrendale, 1998), p. 475.
[6] W. R. Wampler and S. M. Myers, MRS Internet J. Nitride Semicond. Res. **4S1**, G3.73 (1999).
[7] W. Jiang, W. J. Weber, S. Thevuthasan, G. J. Exarhos, and B. J. Bozlee, MRS Internet J. Nitride Semicond. Res. **4S1**, G6.15 (1999).
[8] W. Jiang, W. J. Weber, and S. Thevuthasan, J. Appl. Phys. **87**, 7671 (2000).
[9] A. Wenzel, C. Liu, and B. Rauschenbach, Mater. Sci. Eng., B **59**, 191 (1999).
[10] S. O. Kucheyev, J. S. Williams, C. Jagadish, G. Li, and S. J. Pearton, Appl. Phys. Lett. **76**, 3899 (2000).
[11] S. O. Kucheyev, J. S. Williams, C. Jagadish, J. Zou, M. Toth, M. R. Phillips, H. H. Tan, G. Li, and S. J. Pearton, in *Wide-Bandgap Electronic Devices*, edited by R. J. Shul, F. Ren, M. Murakami, and W. Pletschen, Mater. Res. Soc. Symp. Proc. No. **622** (Materials Research Society, Warrendale, 2000), p. T7.9.1.
[12] S. O. Kucheyev, J. S. Williams, C. Jagadish, J. Zou, and G. Li, Phys. Rev. B **62**, 7510 (2000).
[13] S. O. Kucheyev, J. S. Williams, C. Jagadish, V. S. J. Craig, and G. Li, Appl. Phys. Lett. **77**, 1455 (2000).
[14] S. O. Kucheyev, J. S. Williams, J. Zou, C. Jagadish, and G. Li, Appl. Phys. Lett. **77**, 3577 (2000).
[15] S. O. Kucheyev, J. S. Williams, J. Zou, C. Jagadish, and G. Li, Appl. Phys. Lett. **78**, 1373 (2001).
[16] S. O. Kucheyev, J. S. Williams, J. Zou, J. E. Bradby, C. Jagadish, and G. Li, Phys. Rev. B **63**, 113202 (2001).
[17] S. O. Kucheyev, J. S. Williams, J. Zou, C. Jagadish, and G. Li, Nucl. Instrum. Methods Phys. Res. B **178**, 209 (2001).
[18] S. O. Kucheyev, J. E. Bradby, J. S. Williams, C. Jagadish, M. V. Swain, and G. Li, Appl. Phys. Lett. **78**, 156 (2001).
[19] For a recent review of ion implantation studies in GaN, see, for example, S. O. Kucheyev, J. S. Williams, and S. J. Pearton, Mater. Sci. Eng., R. **33**, 51 (2001).
[20] W. J. Weber, W. Jiang, and S. Thevuthasan, Nucl. Instrum. Methods Phys. Res. B **166-167**, 410 (2000); W. Jiang, W. J. Weber, S. Thevuthasan, and D. E. McCready, J. Appl. Phys. **257**, 295 (1998).
[21] For studies on the formation of hydrogen gas bubbles in H-implanted GaN, see Ref. 6 and S. M. Myers, J. Han, T. J. Headley, C. R. Hills, G. A. Petersen, C. H. Seager, and W. R. Wampler, Nucl. Instrum. Methods Phys. Res. B **148**, 386 (1999); C. H. Seager, S. M. Myers, G. A. Petersen, J. Han, and T. J. Headley, J. Appl. Phys. **85**, 2568 (1999).
[22] It should be noted that the difference in the depth scales of random and aligned spectra (i.e., the difference in the energy loss of analyzing α particles for random and channeling directions) cannot be the reason for such a shift in the position of the bulk RBS/C peak relative to the maximum of the nuclear energy-loss profile. Indeed, such a difference in the depth scales results in an apparent shift of the RBS/C peaks closer to the surface (i.e., to higher energies). This is just the opposite direction of the shift observed in Fig. 1.
[23] K. Schmid, Radiat. Eff. **17**, 201 (1973).
[24] The level of relative disorder of 0.3 has been chosen since (i) the analysis used to extract relative disorder is not valid for very low levels of implantation-produced damage (Ref. 23) and (ii) this level is below the saturation level of damage for all ions used.
[25] J. P. Biersack and L. G. Haggmark, Nucl. Instrum. Methods **174**, 257 (1980).
[26] Calculations of atomic displacements presented in this paper were performed using the TRIM code (Ref. 25). The threshold displacement energy of atoms, E_d, was assumed to be 25 eV for both Ga and N sublattices. To our knowledge, no experimental studies to determine the value of E_d in GaN have been reported in the literature. TRIM simulations (Ref. 25) show that the number of atomic displacements nonlinearly decreases with increasing E_d. However, qualitatively, the results reported in this paper are independent of E_d since the dependence of the ratios of the number of atomic displacements produced by different ions on E_d is negligible for E_d values from 5 to 30 eV.
[27] Note that, due to strong dynamic annealing, ξ_{M_1} is significantly less than unity even for a relatively large value of the threshold displacement energy E_d of 25 eV chosen for TRIM simulations presented here. Lower values of E_d would result in even smaller values for ξ_{M_1}. It can also be noted that, for implantation of Si with heavy ions at low temperatures, ξ_{M_1} is larger than unity due to nonlinear cascade effects and a low level of dynamic annealing, as will be discussed in Sec. IV D.
[28] A legitimate explanation for a low value of ξ_{M_1} in the case of ^{209}Bi ion bombardment (see Fig. 10) is the effect of beam flux previously discussed in Sec. IV A.
[29] It should be noted that, although the number of vacancies generated in the maximum of the nuclear energy-loss profile, N_{vac}^{max}, is larger than the number of vacancies generated at the GaN surface, Fig. 11 still can be used to ascertain the influence of ion mass on the rate of surface amorphization. Indeed, the ratio of N_{vac}^{max} to that value at the surface is compatible for all three ions shown in Fig. 11. A somewhat more accurate analysis would require integration of defect-generation profiles over some distance from the surface or the amorphous/crystalline interface. However, such integration would require knowledge of the parameters describing defect migration and interactions. Unfortunately, at present, not only the numerical values for such parameters but also the dominant defect-interaction processes in GaN are unknown.
[30] See, for example, F. Priolo and E. Rimini, Mater. Sci. Rep. **5**, 319 (1990).
[31] For a recent discussion of the ion-beam-induced amorphous-crystalline phase transition, see, for example, A. I. Titov and S. O. Kucheyev, Nucl. Instrum. Methods Phys. Res. B **168**, 375 (2000), and references therein.
[32] A strong effect of the density of collision cascades on stable implantation damage in GaN discussed here is also supported by our very recent molecular-effect studies, the details of which can be found in S. O. Kucheyev, J. S. Williams, A. I. Titov, G. Li, and C. Jagadish, Appl. Phys. Lett. **78**, 2694 (2001).
[33] See, for example, J. A. Davies, in *Ion Implantation and Beam Processing*, edited by J. S. Williams and J. M. Poate (Academic Press, Sydney, 1984).
[34] For a discussion on the formation of amorphous or highly disordered zones in GaN, see Refs. 12 and 19.
[35] See, for example, J. S. Williams, Rep. Prog. Phys. **49**, 491 (1986), and references therein.
[36] J. P. de Souza, H. Boudinov, and P. F. P. Fichtner, Appl. Phys. Lett. **64**, 3596 (1994); J. P. de Souza, Yu. Suprun-Belevich, H. Boudinov, and C. A. Cima, J. Appl. Phys. **87**, 8385 (2000).